

Model description for single-electron transfer in slow-ion-H₂-molecule collisions: Studies for H⁺, He²⁺, and C⁴⁺ projectiles

Wolfgang Fritsch

Bereich Schwerionenphysik, Hahn-Meitner-Institut Berlin, D-1000 Berlin 39, Germany

(Received 28 April 1992)

We discuss a recently proposed model for describing single-electron transfer in slow- or intermediate-energy-ion-H₂-molecule collisions and present results for the examples of H⁺, He²⁺, and C⁴⁺-ion impact. The dynamics of the two active electrons is given by a one-electron potential model, within the framework of the semiclassical close-coupling description, in conjunction with conservation of the norm of the total two-electron wave function. Considerable numerical simplifications occur when the length of the molecular axis is set to zero. It is argued that this model description of ion-molecule collisions is both efficient and remarkably accurate.

PACS number(s): 34.50.-s, 34.70.+e, 34.10.+x

INTRODUCTION

Theoretical studies of electron processes in heavy-particle collisions at low or intermediate energies have in the past concentrated on one- and two-electron transitions in collisions between atomic or ionic species, and much progress has been achieved in these studies [1,2]. Only a few theoretical investigations have addressed the specific features of collisions involving molecular targets [2]. An example of early work is the schematic model by Bottcher [3] and the Landau-Zener investigation by Olson and Salop [4]. Knudsen, Haugen, and Hvelplund [5] have determined, from the classical Bohr-Lindhard theory, cross-section ratios for highly charged ion impact on H₂ and H targets. A discussion of fast collisions involving molecules is included in the review by McGuire [6].

Very recently, a model for ion-molecule collisions has been proposed [7] which promises to combine the advantage of an efficient one-electron model and the requirement of unitarity conservation. Typically, a consistent one-electron model, when applied to slow-ion-molecule collisions, will lead to one-electron-transition probabilities greater than one, which then need unitarizing in some *ad hoc* fashion [8-10]. On the other hand, a consistent two-electron model for ion-molecule collisions is certainly possible [11], it does conserve unitarity by default but it is very hard and costly to carry through. It is hence an interesting question of how accurate a one-electron description like the one in Ref. [7] can be, and indeed, the reported results [7] for 1s, 2s, and 2p transfer in 1-75 H⁺-H₂ collisions compare reasonably well with data.

In this work, the one-electron description of ion-molecule collisions will be discussed in some detail (see next section). For the purpose of numerical efficiency, it is a key assumption of the theory that the length L of the molecular axis can be set to zero. This assumption is verified by showing, in the subsequent section, results for H⁺-H₂ collisions which are calculated separately with $L=0$ and with $L=1.4$ a.u. [8,9], the value of the equilib-

rium nuclear distance in the H₂ ground-state configuration. Further results, all calculated with the $L=0$ approximation, will be shown for the He²⁺-H₂ and C⁴⁺-H₂ collision systems for which state-specific measurements of electron transfer exist along with similar experimental and theoretical studies for atomic H targets. We will conclude, in the final section, that the proposed efficient, one-electron model of ion-H₂ collisions describes many of the details of measured cross sections when, in the measurements, the initial orientation of the molecular axis is averaged over.

THEORY

To date the most complete description of ion-molecule collisions in the keV energy range is the description of Kimura [11] which has been applied to quasis resonant electron transfer in H⁺-H₂ collisions. This is essentially a consistent two-state, two-electron, three-center model on the basis of the semiclassical close-coupling description.

On the other hand, Shingal and Lin [8,9] have shown that a range of phenomena can be studied very efficiently within a multistate, one-electron three-center model. For each initial orientation of the H₂ molecule, separate collisions are considered between the projectile and each of the hydrogenlike atoms (numbered here as 1 and 2) of the molecule, which are defined by effective nuclear charges of 1.09 and associated 1s wave functions. Separate transition amplitudes $a_n^1(t=+\infty)$ and $a_n^2(t=+\infty)$ for transitions from the initial state at, respectively, center 1 and 2, to projectile state n are determined from solving the coupled equations with atomic basis sets. These amplitudes are then combined, through $A_n = a_n^1 + a_n^2$, to an amplitude A_n for transition from the molecular ground state to the final projectile state n . For the large transition probabilities in slow collisions, $|A_n|$ may take on values up to 2 and hence transition probabilities are deduced from unitarized amplitudes, $\sin|A_n|$.

In this work we use a close-coupling description which starts from a representation of the two-electron wave

function in basis orbitals,

$$\Psi(\mathbf{r}_1, \mathbf{r}_2, t) = \sum_{n=1}^N A_n(t) \phi_n^1(\mathbf{r}_1) \phi_n^2(\mathbf{r}_2), \quad (1)$$

where $\phi_n^i(\mathbf{r}_i)$ denotes a one-electron orbital for electron i (1 or 2) with coordinate \mathbf{r}_i , and the index n lumps all the specifications of the orbital including the center (1, 2, or the projectile) where this orbital is positioned. As we wish to stay within a one-electron potential model *in the critical evaluation of matrix elements*, see below, we adopt as Hamiltonian of the system the single-particle form

$$H = T_1 + V_1 + T_2 + V_2, \quad (2)$$

where T_i denotes the kinetic energy of electron i and $V_i(\mathbf{r}_i)$ the potential affecting the electron with respect to the projectile (effective charge Z_p , position \mathbf{R}_p) and center i (effective charge Z_i , position \mathbf{R}_i),

$$V_i(\mathbf{r}_i) = -\frac{Z_p}{|\mathbf{r}_i - \mathbf{R}_p|} - \frac{Z_i}{|\mathbf{r}_i - \mathbf{R}_i|}. \quad (3)$$

The assumption in Eq. (3) that each electron is affected by the potential of the projectile and only *one* of the two molecular centers would not be strictly necessary for the following but it serves the purpose of staying close to the intuitive picture of separate atomic collisions. It is reflected in any specific choice of basis sets in (1), i.e., electron i should move between the molecular center i and the projectile center only while the other molecular center is shielded, for this electron i , by the other electrons.

Basis expression (1) and the time-dependent Schrödinger equation can now be used as usual [1] to deduce the coupled equations for the amplitudes $A_n(t)$,

$$\sum_{n=1}^N N_{jn}(t) \frac{dA_n(t)}{dt} = i \sum_{n=1}^N M_{jn}(t) A_n(t), \quad j=1, \dots, N \quad (4)$$

with overlap matrix elements

$$N_{jn}(t) = \langle \phi_j^1(\mathbf{r}_1) \phi_j^2(\mathbf{r}_2) | \phi_n^1(\mathbf{r}_1) \phi_n^2(\mathbf{r}_2) \rangle \quad (5)$$

between the two-electron basis states of (1) and corresponding coupling matrix elements

$$M_{jn}(t) = \left\langle \phi_j^1(\mathbf{r}_1) \phi_j^2(\mathbf{r}_2) \left| i \frac{\partial}{\partial t} - H \right| \phi_n^1(\mathbf{r}_1) \phi_n^2(\mathbf{r}_2) \right\rangle. \quad (6)$$

With choice (2), these matrix elements (5) and (6) separate of course into products of one-electron matrix elements. Moreover, there is no coupling between states centered at one of the molecular centers with any of these states centered at the other molecular center.

Hence we arrive at a formulation which uses solely matrix elements as they occur in isolated ion-atom collisions. On the other hand, the use of two-electron wave functions (1), or the use of *joint* amplitudes $A_n(t)$ for the product configurations of both electrons guarantees the conservation of the norm of the wave function. This is in

contrast to the simpler model by Shingal and Lin [8] in which the same one-electron couplings are used as in this work. In Ref. [8], however, completely *separate* amplitudes $a_n(t)$ develop in time for the two electrons and hence the same projectile state may be populated, in an unphysical fashion, by both electrons at the end of the collision. While this feature of the model may be mended to some extent by some *ad hoc* unitarization prescription there is little remedy in the work of [8] against the intermittent population of the same projectile state by both electrons *in course of the collision*.

There is a price to be paid for improving the model description by Shingal and Lin [8]: for studies within the model in this work, we have to solve the close-coupling equations much more often than has to be done in Ref. [8]. We proceed in the following steps.

(a) For a given collision energy and a given basis decomposition (1), we first determine the couplings between one-electron orbitals on a two-dimensional mesh of impact parameters b and scaled times vt (v is the collision velocity). This is done conveniently with methods and codes used for ion-atom collisions [1]. It is only after this step that we turn to the additional features needed for describing ion-molecule collisions.

(b) For a given initial orientation (θ, ϕ) of the molecule and for a given impact parameter vector \mathbf{b} measured from the midpoint of the molecular axis (cf. the geometry considerations of Ref. [8]), we determine, as in [8], separate impact parameters \mathbf{b}_1 and \mathbf{b}_2 for collisions of the projectile with, respectively, molecular centers 1 and 2.

(c) From the set of matrix elements which have been generated for atomic collisions (step 1), we construct by interpolation the matrix elements which are associated with impact parameters b_1 and b_2 . We further transform these matrix elements (which are computed with a choice of coordinate system appropriate for atomic collisions) to their proper form for the choice of coordinate system appropriate for molecular collision, by applying a shift of origin and rotation of axes, cf. Ref. [8].

(d) These matrix elements between one-electron states are then combined with forms (5) and (6) and the coupled equations (4) are solved.

(e) The procedure is repeated, starting from step 2, for a set of initial orientations and a set of impact parameters.

(f) Cross sections are determined as in Ref. [8] after averaging over the initial molecular orientation and summing over impact parameter contributions.

Typically, the main computational burden of the close-coupling method with atomic basis sets lies in the determination of coupling matrix elements rather than the time integration of the coupled equations. The interpolation procedure used for generating the matrix elements for the various initial molecular orientations and impact parameters is hence an important step towards keeping the computational effort for ion-molecule collisions within reasonable limits. We will further specify the model and show results from such calculations for $\text{H}^+ - \text{H}_2$ collision in the next section.

Still, if one is not content with the description of just one leading transfer channel, a multistate expansion in (1)

is needed and then the many time integrations for the set of initial orientations (θ, ϕ) , become a liability. The question then is, how much input about the initial molecular orientation a model really needs when, for comparison with cross-section data, the orientation is averaged over. It has been argued in Ref. [7] that one may start from a complete neglect of the initial orientation, by setting the length L of the molecular axis to zero. This certainly seems justified for the strong, near-resonant transfer channels which determine the total transfer cross section, since at the large impact parameters there will be little effect of the actual displacement between the two molecular centers. But even for the cross sections to the weaker channels which are populated in close collisions, little effect may be left of a finite length L after averaging over orientations and integrating over impact parameters. Indeed, it has been shown in Ref. [7] that the model-sensitive transfer cross sections to H $2p$ and $2s$ states in slow H^+-H_2 collisions, when calculated with the $L=0$ approximation, come out reasonably close to data and distinctively closer than in the work by Shingal and Lin [9]. To our knowledge, no other theory has been tested to that degree. We will show in the next section a direct comparison of results calculated with a length of $L=1.4$ a.u. and 0.

We close this section by noting in compact form a few obvious *shortcomings* of the theory as it has been laid out here. All these shortcomings are linked to the fact that this theory is based on a one-electron model in most of its aspects, except for the time evolution of two-electron product states which in turn is linked to the conservation of unitarity.

(i) This theory does not account for two-electron transfer processes although, in slow collisions, these may considerably contribute to the apparent single-electron transfer cross section.

(ii) In general, the wave function (1) is not symmetric with respect to an exchange of electrons. If it were there would be couplings between states centered at different ends of the molecular axis; this type of couplings would be alien to the concept of quasi-independent atomic collisions. With the additional approximations of $L=0$, however, the representation of the initial H_2 ground state ψ_0 ,

$$\psi_0 = \phi_{1s}^1(\mathbf{r}_1)\phi_{1s}^1(\mathbf{r}_2), \quad (7)$$

with hydrogenic $1s$ orbitals $\phi_{1s}^i(\mathbf{r}_i)$ associated with effective charges of 1.0945, is symmetric.

(iii) In general, the representation of the initial state is not only not symmetric with respect to an exchange of the electrons, more specifically it is also not a product of binding states as it would be in the following choice:

$$\begin{aligned} \psi_0 = \frac{1}{N} \{ & \phi_{1s(1)}^1(\mathbf{r}_1) + \phi_{1s(1)}^1(\mathbf{r}_1) \} \\ & \times \{ \phi_{1s(2)}^2(\mathbf{r}_2) + \phi_{1s(1)}^2(\mathbf{r}_2) \}, \quad (8) \end{aligned}$$

where the additional subscript (i) specifies the molecular center which the associated orbital is attached to and N is a normalization constant. Again, we prefer the form (7) as it is closer to the form required in a model of strictly

one-electron transitions in separate atomic collisions. Actually, with hydrogenic orbitals ϕ_{1s}^1 , as given above and a length of $L=1.4$ a.u. [8], the two forms (7) and (8) have an overlap of 0.86; for $L=0$ they are identical.

Hence there is no question that the theory of this section has a number of features that can be argued against from a standpoint of pure theory. It is solely the search for an efficient and still detailed description of electron-transfer processes in slow-ion-molecule collisions that lets us pursue this model. As it will turn out in the next section, the calculated results indicate that this theory describes experimental cross-section data rather well even to the level of final-state resolved data.

RESULTS AND DISCUSSION

In this section we give for each collision system the specific basis set of traveling atomic orbitals which has been used in the calculations. In all cases, we choose the form (7) as representation of the initial H_2 ground state as explained in the preceding section.

H^+-H_2 collisions

For the benchmark system of H^+-H_2 collisions, we have performed calculations with the length L of the molecular axis chosen as $L=1.4$ a.u. [8,9], and with $L=0$. In the calculation with $L=1.4$ a.u., a basis set of traveling atomic orbitals has been taken which is adapted from the analogous H^+-H collision study [12]. It contains besides the initial state (7), as transfer states, the product states between $1s, \dots, 2p$ projectile (H) states and the $1s, \dots, 2p, 3d$ "united-atom" ($Z=2$) states on one side, with the $1s$ ($Z=1.09$) state at either molecular center 1 or 2 on the other side, i.e., $2 \times 15 = 30$ transfer states. Note the inclusion of pseudostates (tighter bound states of a united atom with $Z=2$) as in [12] which enlarges the basis set but carries promise for satisfactory description of close collisions. In the basis there are also states that are representative of excitation of the molecule: the product of $2s$ and $2p$ (1.09) states and the $1s, \dots, 2p, 3d$ united-atom ($Z=2$) states on center 1 with the $1s$ (1.09) state at center 2, and vice versa, i.e., 28 excitation states. We do not attempt to extract cross sections for excitation of the molecule from the calculations but we believe that some representation of excitation processes is needed if one is to extract the $2s$ and $2p$ capture cross sections in this near-resonant situation. Note that in slow H^+-H collisions, the cross sections for $2s$ and $2p$ capture become identical to, respectively, the $2s$ and $2p$ excitation cross sections, simply because their respective transitions are caused by the same mechanism of couplings between ungerade states [12]. Calculations have been performed for all combinations of polar angles $\theta=0^\circ, 45^\circ, 70^\circ$, and 90° and azimuthal angles $\phi=0^\circ, 45^\circ, 90^\circ, 135^\circ$, and 180° .

Essentially the same basis has been used in the calculations with $L=0$, only that then the number of states is reduced by symmetry. The initial state is symmetric with respect to an exchange of electrons and hence only symmetric combinations of two-electron states need inclusion

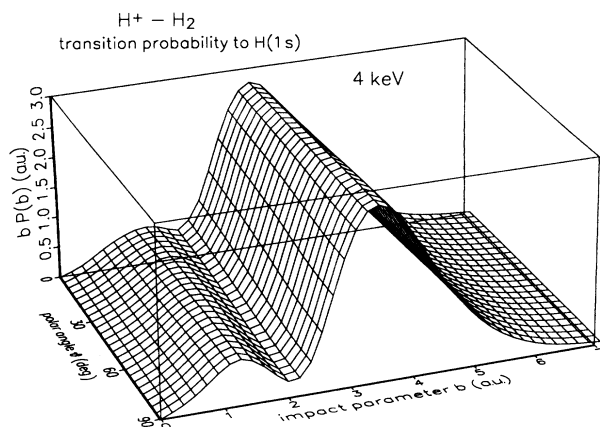


FIG. 1. Calculated dependence of the weighted transition probability $bP(b)$ to the projectile H(1s) state in H⁺-H₂ collisions, on impact parameter and on the polar angle θ of the orientation of the molecular axis. The azimuthal angle ϕ of the orientation is averaged over.

in the basis, e.g., the symmetric sum $\phi_{1s(p)}^1(\mathbf{r}_1)\phi_{1s(2)}^2(\mathbf{r}_2) + \phi_{1s(1)}^1(\mathbf{r}_1)\phi_{1s(p)}^2(\mathbf{r}_2)$ instead of the two separate terms.

In Fig. 1 we show an example of the dependence of the weighted transition probability $bP(b)$ to the projectile H(1s) state on the polar angle θ of the molecular axis, measured against the beam direction as in [8,9], at the energy of 4 keV. For this result, the azimuthal angle ϕ has already been averaged over; the calculated probabilities show a very mild dependence on this angle. As can be seen in Fig. 1, there is very little dependence on θ in the impact-parameter range above 2 a.u. where the main contributions to the total cross section are collected. At lower impact parameters there is some mild dependence on θ . The structure over impact parameter of oscillating probabilities is of course reminiscent of slow H⁺-H collisions.

In Fig. 2 we show a similar dependence for transitions to projectile H(2p) states. As is known from H⁺-H collisions, cf. e.g., [1,2,12], these states are much more weakly populated in slow collisions and the population mecha-

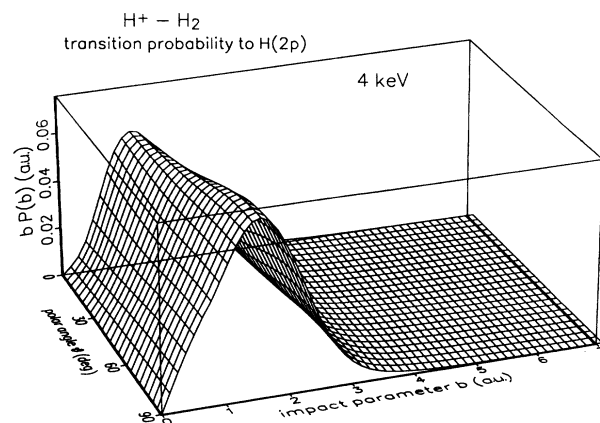


FIG. 2. As in Fig. 1 but for the transition to the projectile H(2p) states.

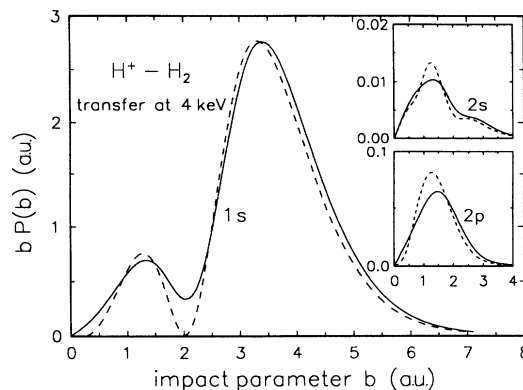


FIG. 3. Calculated weighted transfer probabilities $bP(b)$ in H⁺-H₂ collisions at 4 keV. Full lines denote results from the calculation with a length of $L = 1.4$ a.u. of the molecular axis, after averaging over initial orientations. Dashed lines denote results with a choice of $L = 0$. Note the different scales of the ordinate for 1s, 2p, and 2s transfer states.

nism favors small impact parameters; the same features apply to H⁺-H₂ collisions. Figure 2 shows that the peak in $bP(b)$ is higher and extends to larger impact parameters at 90° than at 0°. This means that for 2p transfer it seems more favorable to have one “atom” pass by closer and the other “atom” at a greater distance (90°) than to have both “atoms” pass by at an intermediate distance (0°). At any rate, the difference does not appear to be very significant.

In Fig. 3 we show the impact-parameter dependence of transfer probabilities to 1s, 2p, and 2s final states at 4 keV, which is computed from the results like those shown in Figs. 1 and 2 by averaging over the polar angle θ . Also in Fig. 3 we show the corresponding result from the calculation with $L = 0$. There turns out to be some difference of results from both types of calculations in the impact-parameter range of 0–2 a.u., but little is left of this difference after integration over impact parameter. Remarkably, this is true not only for total transfer or for the dominant transfer to the H(1s) state but also for the very weak channel or transfer to the H(2s) state. We note that the same observation can be made at two other energies considered, 10 and 1.5 keV.

For all practical purposes therefore it does not appear to make much sense to go through the process of determining orientation-dependent cross sections when, after averaging over orientation, virtually the same results are derived as if one had started from the $L = 0$ approximation in the first place. Still, calculations which include the molecular orientation may be performed if one is interested specifically in effects of the *measurable* molecular orientation, as in molecular collinear explosion after removal of *two* electrons, and we plan to address this question in a future publication [13]. For the purpose of this paper, i.e., for the determination of integrated cross sections for single-electron transfer, the $L = 0$ approximation shall be considered well justified in the context of the present one-electron model of separate atomic collisions.

Figure 4 shows a comparison between transfer probabilities at 4 keV from the present model, with $L = 0$, and

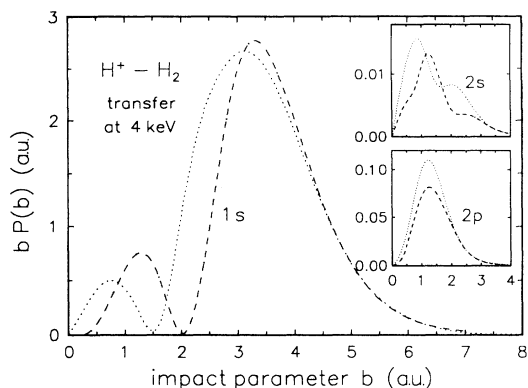


FIG. 4. Calculated weighted transfer probabilities $bP(b)$ in $H^+ - H_2$ collisions at 4 keV. Dashed lines denote results from the model calculations of this work in conjunction with setting $L=0$, as in Fig. 3. Dots denote results that are calculated by assuming completely independent atomic collisions, with $L=0$, and with the unitarization prescription of Ref. [8], cf. text.

transfer probabilities from a model of totally independent atomic collisions, with $L=0$ and with the unitarization prescription of Ref. [8]. For the latter results we first determine atomic collision transition amplitudes a_n as in the $H^+ - H$ study of Ref. [12] but with the target Z replaced by the number 1.0945, and the charge numbers of the associated bound wave functions changed accordingly [note that this is exactly the one-electron basis that is also used in the construction of the two-electron basis (1) in this work, cf. above]. From these amplitudes a_n we then construct transition amplitudes from the molecular initial state to a final state n , by taking $\sin|2a_n|$ in the spirit of Ref. [8].

Figure 4 demonstrates the relative importance of keeping the norm of the two-electron wave function throughout the collision, in contrast to adopting an *a posteriori* unitarization prescription. At large impact parameters, there is virtually no difference of results from both methods, cf. the curve in Fig. 4 for 1s transfer, as would be expected. At the peak of the 1s transfer probability, there is still little difference since, when the probability is close to one, any unitarization prescription will end up with a number close to one. At smaller impact parameters, the probabilities from both methods may, however, become quite different. This would result in little difference of calculated total transfer cross sections, 15% for the example of Fig. 4. The calculated small transfer cross sections to 2p and 2s states, on the other hand, are different, between the two methods, as the impact parameters for their population are small. In the example of Fig. 4, the difference is in the 30(2p)–40(2s) % range but probably it may become even larger in other cases, e.g., in cases when a few transfer states are populated about equally while the total transfer probability adds up to 1. Typically this is the case for collisions with highly charged ions.

In Fig. 5, the calculated 2p transfer cross sections from this work, with $L=0$, are compared to the results derived earlier with a larger basis set [7], to the data by Andreev, Ankudinov, and Bobashev [14] and by Birley and

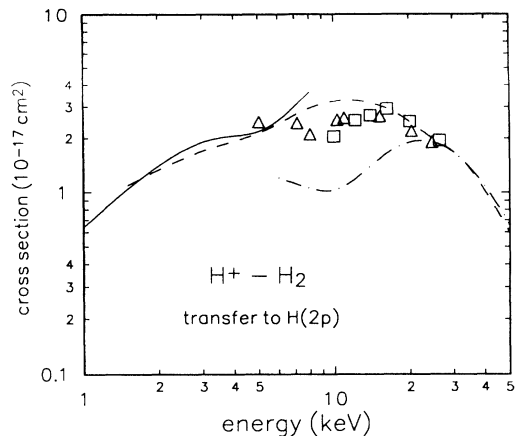


FIG. 5. Calculated transfer cross sections to $H(2p)$ states in $H^+ - H_2$ collisions from this work with $L=0$ (full line), from similar work with a larger basis set [7] (dashed line), and from the work by Shingal and Lin [9] (dash-dotted line). Data are by Andreev, Ankudinov, and Bobashev [14] (\square), and by Birley and McNeal [15] (\triangle).

McNeal [15], and to the calculated cross sections by Shingal and Lin [9]. The calculated results from this work and the earlier model calculations [7] agree well at low energies, thus showing that the smaller basis choice in this work is appropriate at those energies. Above 7 keV, the results from this work start deviating from the cross sections of Ref. [7]. It is there that pseudocontinuum states are needed as they are included in Ref. [7], cf. the similar arguments in work on $H^+ - H$ collisions at higher energies [16]. The results from the model of this work and Ref. [7] are seen to agree well with the data; they seem to do better than the results by Shingal and Lin [9]. We note that the latter results would probably be improved if, in the model of Ref. [9], a larger basis set were taken.

We do not show here the calculated results for electron transfer to $H(1s)$ and $H(2s)$ states but refer to Ref. [7]. Also for these final states, the results from this work agree well with those from Ref. [7] which are derived with a larger basis set. For $H(2s)$ production above 7 keV, the cross sections from this work again deviate from the result shown in Ref. [7], for reasons given above.

$He^{2+} - H_2$ collisions

The $He^{2+} - H_2$ collisions, electron transfer is known to populate mainly the $He^+(n=2)$ states, similarly as in the $He^{2+} - H$ system [1,17–19]. For the close-coupling calculations with the $L=0$ assumption, we have chosen a basis which includes, besides the initial state, the $n=2$ capture states as products of the $He^+(n=2)$ states with the 1s (1.0945) state of the remaining electron at the location of the molecule. Also pseudostates have been included in the basis: products of the 3d (3.0) states at the He center with the 1s (1.0945) state at the molecule, and products of the 2s, 2p, 3d (3.0) states with the 2s (1.0945) state, both centered at the molecule. The choice of pseudostates is guided by the molecular orbital (MO) energy diagram for

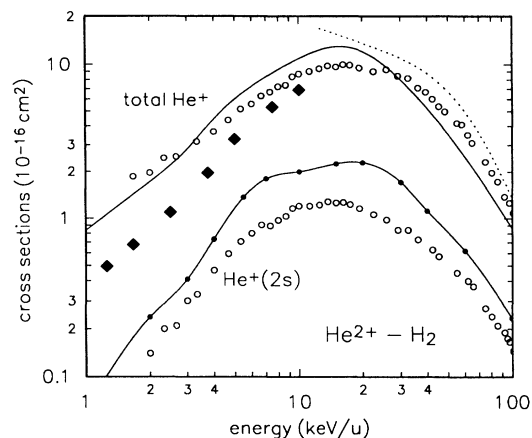


FIG. 6. Calculated transfer cross sections in $\text{He}^{2+}\text{-H}_2$ collisions from this work (full lines) are compared to the data by Shah and Gilbody [20] (circles), and to cross sections calculated by Shingal and Lin [8] (dotted line). The upper pair of results are for total He^+ production, the lower pair for $\text{He}^+(2s)$ production. The diamonds designate measured cross sections for $\text{He}^+(2p)$ production by Cirić *et al.* [17].

the $(\text{He-H})^{2+}$ system [1], which shows that the set of initial state and main transfer states correlates, at small internuclear separations, to the set of the $n=2$ and $3d$ states of the united atom ($Z=3$).

In Fig. 6, the calculated transfer cross sections for this collision system are compared to data and to cross sections determined by Shingal and Lin [8]. The measured total He^+ production by Shah and Gilbody [20] is seen to agree well with the calculated total single-electron transfer over the whole of the considered energy range, and so do the results by Shingal and Lin. On the other hand, for the weak channel of electron transfer to the $\text{He}^+(2s)$ state there is some difference between data and calculated results, of up to 50% at the maximum. Still, even for this weak channel, the general shape of the two sets of results is very similar.

The difference in absolute magnitude between results for the $\text{He}^+(2s)$ channel may appear to be somewhat surprising despite the weakness of this channel. We have tried a number of other, enlarged basis sets in calculations for this system and found the calculated cross sections to the $\text{He}^+(2s)$ state to be rather stable against variations of the basis. On the other hand, the indicated difference may not necessarily indicate that the general model is only accurate to that degree. For $\text{He}^{2+}\text{-H}$ collisions, a very similar discrepancy has been well known over the years; it has only recently been resolved by the measurements of Cirić *et al.* [17], see also the discussion in Ref. [1].

The calculated total single-electron transfer cross section is determined, due to the basis choice, as a cross section for population of mainly $\text{He}^+(2p)$ states. At higher energies, one may argue that the calculated transfer cross sections implicitly include cross-section contributions to higher states that are not included in the basis. At energies below 10 keV, however, the data by Cirić *et al.*, for direct $\text{He}^+(2p)$ population (cf. Fig. 6) show that the ex-

perimental cross sections for total He^+ production from Ref. [20] include contributions from other processes, such as capture to $\text{He}^+(1s)$ in conjunction with dissociation of the molecule; see the discussion in Refs. [17,18]. The good agreement between data by Shah and Gilbody and the results of this work would then indicate that these other processes draw their flux from the $\text{He}^+(2p)$ channel. In other words, in slow collisions, total single-electron transfer is associated with large transition probabilities and hence the neglect of any particular transfer process may not significantly change the calculated transfer cross section.

In Fig. 7 the ratio of single-electron transfer cross sections for $\text{He}^{2+}\text{-H}_2$ and $\text{He}^{2+}\text{-H}$ collisions is taken from the data by Shah and Gilbody [20] and displayed in comparison with ratios from calculations for the H_2 target, this work, and calculations for the H target [21]. Also the ratio from the calculation by Shingal and Lin [8] is shown. Because the calculations of this work include, in an explicit manner, only the $\text{He}^+(n=2)$ transfer states we show two sets of calculated ratios: for one ratio, we take the cross sections for $\text{He}^+(n=2)$ population in collisions with H [21], for the other we take the total transfer cross section in collisions with H [21] [this includes the $\text{He}^+(n=1-7)$ states]. One may argue that the former choice is more reasonable since, at higher energies, the $\text{He}^+(n=2)$ population is representative for a certain portion of the total transfer cross section, almost the same portion for H_2 or H targets. On the other hand, one may argue that the calculated transfer cross sections from this work, at the higher energies, include implicitly contributions to higher- n states so that they should be combined with the *total* transfer cross sections from Ref. [21]. The comparison with the data in Fig. 7 indicates that the former argument is better justified than the latter. This

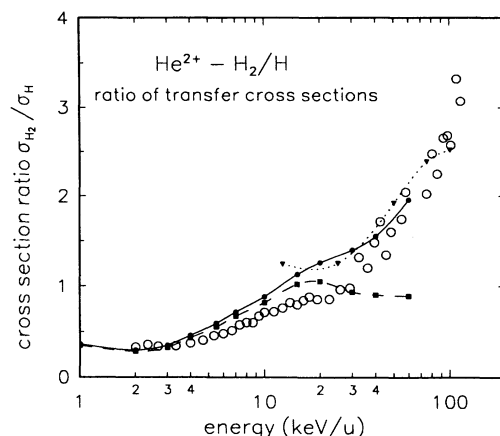


FIG. 7. Ratio of total single-electron transfer cross sections for $\text{He}^{2+}\text{-H}_2$ and $\text{He}^{2+}\text{-H}$ collisions from Shah and Gilbody [20] (circles), from the AO model calculation by Shingal and Lin [8] (dotted line), and from this work in conjunction with the calculated $\text{He}^{2+}\text{-H}$ cross sections from Ref. [21] (solid and dashed lines). For the upper (solid) curve, the cross section for $\text{He}^+(n=2)$ production in collisions with H is taken from Ref. [21], for the lower (dashed) curve and summed cross section for $\text{He}^+(n=1-7)$ production is taken.

means that with a larger basis set for the $\text{He}^{2+}\text{-H}_2$ system, the calculated total transfer cross section may be larger than in this work, by up to a factor of 2 at the high energies. This would still be in good accord with the data for total He^+ production, see Fig. 6. We note that the ratio from the simpler atomic-orbital- (AO-) type model by Shingal and Lin [8] is very close to the results from this work. Only at its low-energy end around 10 keV does the curve from Ref. [8] show a different trend. One may speculate that the simple AO basis taken in Ref. [8], which does not include pseudostates, becomes less appropriate at low energies. Also the *ad hoc* unitarization procedure adopted in Ref. [8] may limit the accuracy of results.

From Fig. 7 we note that the plotted cross-section ratio has no association to anything close to 2, in contrast to what one would naively expect. It is also smaller, at low energies, than what has been noted [5] as an average, near-universal value (0.8) for collisions with more highly charged projectiles ($q > 4$).

$\text{C}^{4+}\text{-H}_2$ collisions

For the investigation of $\text{C}^{4+}\text{-H}_2$ collisions, the projectile potential in Eq. (3) has been replaced by an exponentially screened Coulomb potential, the same that has been used successfully in an investigation of $\text{C}^{4+}\text{-H}$ collisions [22]. The basis set, within the $L=0$ approximation, has to be chosen in such a way that its orbitals represent the $\text{C}^{3+}(n=3)$ states. Specifically, we chose a set of hydrogenic ns states at the projectile center which consist of $1s$ (8.00), $2s$ (4.53), $3s$ (4.44), $1s$ (5.11), and $1s$ (1.78) states, $2p$ (4.89), $3p$ (3.98), and $2p$ (2.66) states, and of $3d$ (4.01) states. The carbon potential is diagonalized in this basis set and the lowest energies and associated eigenvectors are taken as the lowest physical energies and representations of the states of the system after capture (the charge parameters of the basis states are determined by a minimization procedure for the energies); see also the similar procedure in Ref. [22].

For the two-electron basis in Eq. (1), these one-electron capture states are multiplied by the set of $1s$ (1.0945), $2s$ (5.0), and $2p$ (5.0) states at the hydrogen center. At the position of the molecule, we include the products of the $n=2$ and 3 states (charge parameter 5.0) with the $1s$ (1.0945) state besides the initial state. The choice of "united-atom" orbitals (charge parameter 5.0) in this basis does not include all the states that one would wish to adopt; the adoption of the full set of $n=2-4$ united-atom orbitals [22] was deemed too costly in the context of this study.

In Fig. 8 the calculated transfer cross sections to the $\text{C}^{3+}(n=3)$ states and their l distribution are displayed and compared to data by Dijkkamp *et al.* [23], by Hoekstra *et al.* [18,24], and by Goffe, Shah, and Gilbody [25]. The calculated transfer cross sections to the set of $n=3$ states is seen to be slightly larger, by some 20% than the data below 10 keV/u; apparently the difference lies mainly in a discrepancy with respect to the $3s$ state. On the whole the agreement between the calculated and measured cross sections is deemed very satisfactory. We

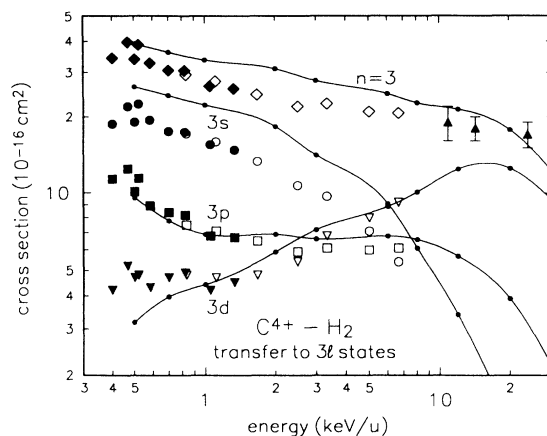


FIG. 8. Electron transfer cross sections to $\text{C}^{3+}(n=3)$ states in $\text{C}^{4+}\text{-H}_2$ collisions. Calculated results from this work (full lines) are compared to data by Dijkkamp *et al.* [23] (closed symbols; circles for $3s$, squares for $3p$, inverted triangles for $3d$, and diamonds for total $n=3$ population), by Hoekstra *et al.* [18,24] (open symbols), and by Goffe, Shah, and Gilbody [23] (closed triangles with error bars for total transfer).

note that the low-energy data shown in Fig. 8 have been confirmed in very recent measurements by McLaughlin, McCullough, and Gilbody [26]. The l distribution of transfer cross sections is also in harmony, at their low-energy end, with the calculations by Gargaud and McCarroll [27] which extend up to 0.25 keV/u. Those calculations are based on a fully one-electron potential model with molecular orbitals.

In Fig. 9 ratios of transfer cross sections for $\text{C}^{4+}\text{-H}_2$ and $\text{C}^{4+}\text{-H}$ collisions are displayed. They have been taken from the experimental work by Phaneuf *et al.* [28], by Crandall, Phaneuf, and Meyer [29], and by Goffe, Shah, and Gilbody [25], and from this work (cross sections for

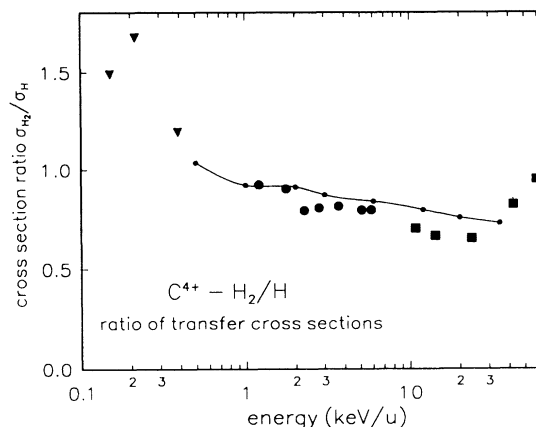


FIG. 9. Ratio of single-electron transfer cross sections for $\text{C}^{4+}\text{-H}_2$ and $\text{C}^{4+}\text{-H}$ collisions. Experimental ratios are taken from work by Phaneuf *et al.* [28] (inverted triangles), by Crandall, Phaneuf, and Meyer [29] (circles), and by Goffe, Shah, and Gilbody [25] (squares). The solid line is the result of taking the ratio of cross sections from this work for the H_2 target and the cross sections from Ref. [22] for the H target.

H₂) in conjunction with Ref. [22] (cross sections for H). There is good consistency within the data, and close agreement between the calculation and the data. At the highest energies, the calculated curve fails to show increasing ratios as the data do. A possible explanation may be the missing contributions of transfer to the $n = 4$ states in the calculations of this work. The mean value of the ratio between 1 and 10 keV is close to the low-energy plateau in the universal curve given by Knudsen *et al.* [5] for charge states $q > 4$. In that universal curve, however, there is no indication for an increase of the ratio, with decreasing energy, below 1 keV.

CONCLUSIONS

In this work we test a three-center, multistate close-coupling model for describing one-electron transfer in H⁺-H₂ collisions. This model starts from a two-electron wave function and hence avoids any *a posteriori* unitarization prescription. On the other hand, the coupling matrix elements in this model are those of two independent collisions between the ion and the two atomic constituents of the molecule. In spite of the simplicity of the model, we find good agreement between the results of this model and data, even for the weak, sensitive channel of transfer to H(2*p*) states.

An even simpler model emerges when the length L of the molecular axis is set deliberately to zero. For the H⁺-H₂ collision system, we find that the additional approximation of $L = 0$ leads only to very minor modifications of calculated results when, in the case of results from the three-center ($L = 1.4$ a.u.) description, the initial orientation of the molecule is averaged over.

The proposed model in conjunction with setting $L = 0$ is tested for He²⁺-H₂ and for C⁴⁺-H₂ collisions. Calculated total and substate transfer cross sections are found to agree with data typically within 20%, except for the case of He⁺(2*s*) population where the experiment may have large uncertainties, similar to what has been found recently for H targets. Also calculated ratios of transfer cross sections with H₂ and H targets turn out to agree well with corresponding ratios of data.

We hence believe that the proposed model provides for a very efficient means to investigate collisions between ions and H₂ molecules in the energy range of the applicability of the close-coupling method. Problems may occur at low energies in cases when two-electron processes are important. In situations which are governed by single-electron processes, this model may point the way towards efficient, detailed descriptions of collisions between ions and molecules, or, more generally, collisions with complex atomic aggregates.

-
- [1] W. Fritsch and C. D. Lin, *Phys. Rep.* **202**, 1 (1991).
 [2] M. Kimura and N. F. Lane, *Adv. At. Mol. Opt. Phys.* **26**, 79 (1990).
 [3] C. Bottcher, in *Coherence and Correlation in Atomic Collisions*, edited by H. Kleinpoppen and J. F. Williams (Plenum, New York, 1980), p. 403.
 [4] R. E. Olson and A. Salop, *Phys. Rev. A* **14**, 579 (1976).
 [5] H. Knudsen, H. K. Haugen, and P. Hvelplund, *Phys. Rev. A* **24**, 2287 (1981).
 [6] J. H. McGuire, *Adv. At. Mol. Opt. Phys.* **29**, 217 (1992).
 [7] W. Fritsch, *Phys. Lett. A* **166**, 238 (1992).
 [8] R. Shingal and C. D. Lin, *Phys. Rev. A* **40**, 1302 (1989).
 [9] R. Shingal and C. D. Lin, *J. Phys. B* **22**, L659 (1989).
 [10] M. Kimura, *Phys. Rev. A* **33**, 4440 (1986).
 [11] M. Kimura, *Phys. Rev. A* **32**, 802 (1985).
 [12] W. Fritsch and C. D. Lin, *Phys. Rev. A* **26**, 762 (1982).
 [13] W. Fritsch (unpublished).
 [14] E. P. Andreev, V. A. Ankudinov, and S. V. Bobashev, in *Proceedings of the 5th International Conference on the Physics of Electronic and Atomic Collisions* (Nauka, Leningrad, 1967), p. 309.
 [15] J. H. Birley and R. J. McNeal, *Phys. Rev. A* **5**, 692 (1972).
 [16] W. Fritsch and C. D. Lin, *Phys. Rev. A* **27**, 3361 (1983).
 [17] D. Cicić, D. Dijkkamp, E. Vlieg, and F. J. de Heer, *J. Phys. B* **18**, 4745 (1985).
 [18] R. Hoekstra, Ph.D. thesis, Rijksuniversiteit Groningen, 1990.
 [19] R. Hoekstra, F. J. de Heer, and R. Morgenstern, *J. Phys. B* **24**, 4025 (1991).
 [20] M. B. Shah and H. B. Gilbody, *J. Phys. B* **11**, 121 (1978).
 [21] W. Fritsch, *Phys. Rev. A* **38**, 2664 (1988).
 [22] W. Fritsch and C. D. Lin, *J. Phys. B* **17**, 3271 (1984).
 [23] D. Dijkkamp, D. Cirić, E. Vlieg, A. de Boer, and F. J. de Heer, *J. Phys. B* **18**, 4763 (1985).
 [24] R. Hoekstra, J. P. M. Beijers, A. R. Schlatmann, and R. Morgenstern, *Phys. Rev. A* **41**, 4800 (1990).
 [25] T. V. Goffe, M. B. Shah, and H. B. Gilbody, *J. Phys. B* **12**, 3763 (1979).
 [26] T. K. McLaughlin, R. W. McCullough, and H. B. Gilbody, *J. Phys. B* **25**, 1257 (1992).
 [27] M. Gargaud and R. McCarroll, *J. Phys. B* **18**, 463 (1985).
 [28] R. A. Phaneuf, I. Alvarez, F. W. Meyer, and D. H. Crandall, *Phys. Rev. A* **26**, 1982 (1982).
 [29] D. H. Crandall, R. A. Phaneuf, and F. W. Meyer, *Phys. Rev. A* **19**, 504 (1979).